



저작자표시-비영리-변경금지 2.0 대한민국

이용자는 아래의 조건을 따르는 경우에 한하여 자유롭게

- 이 저작물을 복제, 배포, 전송, 전시, 공연 및 방송할 수 있습니다.

다음과 같은 조건을 따라야 합니다:



저작자표시. 귀하는 원저작자를 표시하여야 합니다.



비영리. 귀하는 이 저작물을 영리 목적으로 이용할 수 없습니다.



변경금지. 귀하는 이 저작물을 개작, 변형 또는 가공할 수 없습니다.

- 귀하는, 이 저작물의 재이용이나 배포의 경우, 이 저작물에 적용된 이용허락조건을 명확하게 나타내어야 합니다.
- 저작권자로부터 별도의 허가를 받으면 이러한 조건들은 적용되지 않습니다.

저작권법에 따른 이용자의 권리는 위의 내용에 의하여 영향을 받지 않습니다.

이것은 [이용허락규약\(Legal Code\)](#)을 이해하기 쉽게 요약한 것입니다.

[Disclaimer](#)

이학석사 학위논문

연못 퇴적토 속 자철석 입자에  
착생하는 미생물 군집에 관한 연구

Distinctive Microbial Community Associated  
with Pond Sediment Magnetite Grains

2016 년 2 월

서울대학교 대학원

생명과학부

송 호 경

연못 퇴적토 속 자철석 입자에 착생하는

미생물 군집에 관한 연구

Distinctive Microbial Community  
Associated with Pond Sediment  
Magnetite Grains

지도 교수 Jonathan Miles Adams, Ph.D.

이 논문을 이학석사 학위논문으로 제출함

2016 년 2 월

서울대학교 대학원

생명과학부

송 호 경

송호경의 이학석사 학위논문을 인준함

2016 년 2 월

위 원 장 이 은 주 (인)

부위원장 Jonathan Adams (인)

위 원 Piotr Jablonski (인)

# Distinctive Microbial Community Associated with Pond Sediment Magnetite Grains

Hokyung Song

Advisor: Professor Jonathan Adams, Ph. D.

A Thesis Submitted for the Partial Fulfillment of the  
Degree of Master of Science, Biological Sciences

February 2016

Graduate School of Biological Sciences  
Seoul National University

# Abstract

Magnetite is a naturally occurring ferrimagnetic mineral. It can be formed by both abiotic and biotic processes. Biological magnetite formation through dissimilatory iron reduction has been well-studied in culture since those bacterial species that perform dissimilatory iron reduction have various applications. However, from an ecological perspective, their presence and role as a magnetite former in natural environments are unclear. In this study, bacteria associated with magnetite grains from freshwater pond sediment were investigated. Pond sediment samples were collected and subjected to magnetic separation, enriching magnetite grains while leaving magnetite-depleted fraction behind. Soil DNA was taken from each of the magnetite-enriched and magnetite-depleted samples, and the V3 region of bacterial 16S ribosomal RNA (rRNA) gene was amplified. Using next generation sequencing (NGS) technique, bacterial community structure of the magnetite-enriched fraction was compared to that of the magnetite-depleted fraction. In the magnetite-enriched fraction, the most abundant operational taxonomic unit (OTU) belonged to *Geobacter*, a genus known to include several species that can form magnetite in culture condition. There were several other bacterial species particularly abundant in the magnetite-enriched fraction, inviting further investigation of their potential contribution to magnetite formation in nature. Overall, bacterial community structure of the magnetite-enriched and magnetite-depleted fractions was distinct from each other,

providing a glimpse towards understanding how bacterial diversities in sediments and soils are structured and how a variety of bacterial species can coexist in soils.

**Keyword:** magnetite, *Geobacter*, next generation sequencing (NGS), niche differentiation, bacterial 16S ribosomal RNA (rRNA) gene

**Student Number:** 2014–20313

# List of Figures

<b>Fig. 1</b>	Representative figure of magnetic separation process.....	8
<b>Fig. 2</b>	Representative figure of magnetite–enriched (left) and magnetite–depleted (right) sample .....	9
<b>Fig. 3</b>	Typical XRD pattern observed for pond sediment showing the presence of magnetite and hematite phase in pond sediment. A small fraction of oxidized form of magnetite and maghemite is also visible possibly due to surface oxidation of magnetite during the washing of sediment by ethanol.....	17
<b>Fig. 4</b>	Scanning ion micrographic image of sediment a indicating the spiral step growth along (111) crystallographic direction as suggested by the triangular morphology. b The encircled section subject to FIB cross–section cutting is shown in the inset Fig (e) indicatinv the presence of defects between the two steps. c The HRTEM micrograph showing the lattice presence typical of a crystal structure. d FFT of square section of c indicating the stacking of (111) type planes.....	18
<b>Fig. 5</b>	Phylum breakdown of magnetite–enriched and magnetite–depleted group .....	21
<b>Fig. 6</b>	Rarefaction curve showing species accumulation rate of magnetite–enriched and magnetite–depleted group .....	22
<b>Fig. 7</b>	nMDS plot showing taxonomic distance between each sample .....	23
<b>Fig. 8</b>	Heatmap showing the relative abundance of the 50 most abundant OTUs.....	24

**Fig. 9** qPCR result for 16S gene copy number (a measure of bacterial cell abundance) of bulk sediment group and magnetite-enriched group..... 25

# List of Tables

<b>Table 1</b> Magnetic intensity required for magnetic separation of minerals.....	<b>3</b>
<b>Table 2</b> Indicator species of magnetite–depleted (D) and magnetite–enriched (M) group among top 500 OTUs .....	<b>26</b>
<b>Table A1</b> Functional characterization of magnetite–depleted (D) and magnetite–enriched (M). Only the top 50 most dominant functions are shown .....	<b>52</b>

# Table of Contents

Abstract .....	i
List of Figures .....	iii
List of Tables .....	v
Table of Contents.....	vi
<b>1. Introduction .....</b>	<b>1</b>
1.1. Magnetite and its formation.....	1
1.2. Research objectives.....	4
<b>2. Materials and Methods.....</b>	<b>6</b>
2.1. Sample collection .....	6
2.2. Magnetic separation.....	6
2.3. DNA extraction and PCR amplification.....	10
2.4. Sequencing and sequence processing .....	10
2.5. Statistical analysis .....	11
2.6. Structural and microstructural configuration of magnetically-enriched fraction .....	12
2.7. Quantitative PCR analysis .....	13
<b>3. Result .....</b>	<b>15</b>
3.1. Presence and Microstructure of Magnetite in the magnetically-enriched fraction .....	15
3.2. Bacterial community structure of magnetite-enriched fraction	19
<b>4. Discussion .....</b>	<b>36</b>
4.1. Greater relative abundance of <i>Geobacter</i> in magnetite-	

enriched group.....	36
4.2. Micro-scale niche partitioning.....	37
5. Conclusions.....	40
Publication.....	41
Bibliography.....	42
APPENDIX.....	47
국문초록 (Abstract in Korean).....	55

## 일러두기

본 논문은 학술지 *Microbial Ecology* 에 2015년 1월 발표된 논문 “Pond Sediment Magnetite Grains Show a Distinctive Microbial Community”를 석사학위 논문으로 발전시킨 것이다.

# 1. Introduction

## 1.1. Magnetite and its formation

Magnetite is a ferrous–ferric oxide with the formula,  $\text{Fe}_3\text{O}_4$ . It is a commonly occurring mineral on Earth, being widely distributed, mainly in the terrestrial environment (Jimenez-Lopez et al., 2010). It possesses a ferrimagnetic property, which is similar to the ferromagnetic property except that they have different alignment of electron spin (Néel, 1955). Both ferrimagnetic minerals and ferromagnetic minerals are more strongly magnetic than other types of minerals such as diamagnetic or paramagnetic minerals in that they can show magnetic properties even when magnetic fields are not applied. For this reason, magnetite can be extracted more easily than other naturally occurring minerals by magnetic induction (Table 1, (Morgan, 2000))

Magnetite can be formed both abiotically and biotically. Abiotic magnetite formation includes the “coprecipitation” method, which can be conducted under anoxic conditions in solutions containing  $\text{Fe(II)}$  and  $\text{Fe(III)}$ , and the “reduction–precipitation” method, which occurs in a solution that has only  $\text{Fe(III)}$  as an iron source (Jimenez-Lopez et al., 2010). Biotic magnetite formation, which can also be called biomineralization, occurs in two ways: 1) biologically controlled mineralization (BCM) and 2) biologically induced mineralization (BIM) (Bazylinski et al., 2007; Jimenez-Lopez et al., 2010).

BCM is performed by magnetotactic bacteria, which have magnetite inside the cell for the purpose of orienting itself to the earth magnetic field (Blakemore, 1975). This process is known to be precisely controlled by gene regulation, and the magnetite produced has relatively regular size and structure compared to magnetite that has been formed by BIM (Bazylinski et al., 2007; Jimenez-Lopez et al., 2010). BIM, on the other hand, is performed by organisms that use Fe(III) as a terminal electron acceptor in their electron transfer chain (Bazylinski et al., 2007; Lovley, 2013). These organisms are called dissimilatory iron reducing bacteria, and the best known bacteria in this group is *Geobacter*, which forms magnetite in a culture condition by oxidizing organic matter and reducing Fe(III) (Lovley, 2013; Lovley et al., 1987).

**Table 1** Magnetic intensity required for magnetic separation of minerals (Morgan, 2000)

Mineral	Magnetic intensity, T <sup>a</sup>	Mineral	Magnetic intensity, T <sup>a</sup>
alabandite	1.5 – 1.8	limonite	1.6 – 2.0
ankerite	>1.3 – <1.6	maghemite	0.3 – 0.5
apatite	1.4–1.8	<b>magnetite</b>	<b>&lt;&lt;0.1</b>
bastnasite	1.5–1.7	martite	0.2 – 0.6
biotite	1.0–1.8	monazite	<1.4 – 2.0
braunite	1.4–1.8	muscovite	1.5 – 2.3
chromite	1.0–1.6	olivine (fayalite)	1.1 – 1.5
chrysocolla	2.0–2.4	pyrochlore	1.2 – 1.6
columbite	1.2–1.6	pyrolusite	1.5 – 1.9
columbite– tantalite	1.2–1.6	pyrrhotite	0.1 – 0.4
dauidite	1.2–1.6	renierite	1.4 – 1.8
epidote	>1.4 – 2.0	rhodochrosite	1.5 – 2.0
euxenite	1.6 – 2.0	rhodonite	1.5 – 2.0
ferberite	>0.1 – 0.4	samarskite	1.6 – 2.0
franklinite	<0.3 – <0.5	siderite	<1.0 – 1.8
garnet	1.2–1.0	staurolite	1.2 – 1.9
goethite	1.5–1.8	serpentine	>0.4 – >1.8
haematite	>1.3 – 2.0	tantalite	1.2 – 1.7
hornblende	>1.6 – 2.0	titaniferrous magnetite	<0.1 – 0.3
ilmenite	0.8 – 1.6	tourmaline	1.6 – 2.0
ilmenorutile	1.5 – 1.8	uraninite	1.8 – 2.4
itabirite	0.8 – <1.4	wolframite	1.2 – 1.6
		xenotime	1.1 – 1.6

## 1.2. Research objectives

Studying groups of bacteria that may be involved in magnetite formation is an active area of research in applied biotechnology. For example, magnetite produced by magnetotactic bacteria is small in their size and safer than artificially formed ones, so can be used for medical purposes, such as magnetic resonance imaging (MRI) (Goldhawk et al., 2012). Dissimilatory iron reducing bacteria can be used for bioremediation of metal-contaminated waste waters (Lovley, 1995). Therefore, there has been many studies trying to discover novel magnetite formers, culture those, and develop techniques focusing on their potential usages (Byrne et al., 2011; Greene et al., 1997; Nevin et al., 2005). However, their performance from an ecological perspective, whether they play a role out in nature as a magnetite former, is still unknown. If it is possible to demonstrate their physical association with magnetite grains, this would bolster the case that they are indeed important in magnetite formation in nature.

By applying culture independent methods, it may also be possible to find previously undescribed species which have a physical association with magnetite grain. Although this is not enough to categorically state that they are magnetite formers, it could be the first step towards finding a novel candidate species that may play a role in magnetite formation.

In this study, using a powerful rare earth magnet, magnetite grains were separated from bulk sediment soils leaving “magnetite–

depleted” soils behind. In a more general perspective of microbial ecology, comparing microbial community structure of magnetite-enriched soils against that of magnetite-depleted soil, would help us to understand how tens of thousands of bacterial species coexists in a gram of soil. This was one of the major questions after the development of next generation sequencing (NGS) (Vos et al., 2013).

This study was designed to test the following hypotheses related to the topics mentioned above.

1. That certain bacterial species known to form magnetite in culture, for instance *Geobacter*, will be relatively more abundant in the magnetite-enriched fraction compared to magnetite-depleted fraction
2. That there will be previously uncultured forms of bacteria enriched in magnetite-enriched fraction compared to magnetite-depleted fraction inviting further investigation of their potential contribution as a magnetite former in nature.
3. Bacterial community structure of magnetite-enriched fraction will be distinct from that of magnetite-depleted fraction implying niche differentiation occurring in micro-scale and providing one explanation for the question how soil bacterial diversity is structured.

## 2. Materials and Methods

### 2.1. Sample collection

Samples were collected in a freshwater pond which has been located in the campus of Seoul National University, South Korea (37°27'38.3"N, 126°57'07.5"E). The pond was constructed artificially more than 30 years ago in a pre-existing upland stream course. The size of the pond is about 0.25 Hectare in area, and around 1 m deep in average, with aquatic vegetation.

Pond sediment samples were collected at 4 points with 1 m spacing. All of the samples were collected at the same date in late June. At each sampling point, top 5cm sediment soils were cleared out and 5 to 15cm depth soils were collected. Pond sediment redox potential was measured with pH-meter connected portable platinum electrode (Faulkner et al., 1989; Vo and Kang, 2013). Values got from two measurements of redox potential was 311–319 mV vs. standard hydrogen electrode (SHE) at depth 6 cm and 341–347 mV vs. SHE.

### 2.2. Magnetic separation

200 g of sediment from each sampling point were placed in a glass beaker filled with distilled water and gently shaken while a strong rare earth magnet with a magnetic force of 0.4 Tesla, was placed outside of the edge of the beaker. The black material stuck in the side of the beaker close to the magnet, were collected with clean spatula and placed inside a 50-mL Falcon tube. The magnet

was placed on one side of the Falcon tube filled with distilled water and were shaken (Fig. 1). The same suspension process was repeated until no more magnetic mineral could be obtained. The purified blackish magnetic mineral was kept as “magnetically-enriched” sample (Fig. 2). The remaining sediment in the 50-mL Falcon tube with no more magnetic mineral were yellowish in its color (Fig. 2). The remained soil was kept as “magnetically-depleted” sample.



**Fig. 1** Representative figure of magnetic separation process



**Fig. 2** Representative figure of magnetite-enriched (left) and magnetite-depleted (right) sample

### 2.3. DNA extraction and PCR amplification

Soil DNA from magnetically-enriched and magnetically-depleted samples were extracted using Power Soil DNA extraction kit (MoBio Laboratories, Carlsbad, CA, USA) following the manufacturer's instruction. V3 region of bacterial 16S rRNA gene was amplified with universal bacterial primer 338F (5'-XXXXXXXX-YY-GTACTCCTACGGGAGGCAGCAG-3') and 533R (5'-XXXXXXXX-YY-TTACCGCGGCTGCTGGCAC-3') while X denotes barcode sequence and Y denotes adaptor sequence. The PCR condition was as follows: 1) pre-denaturation step at 94 °C for 2 min, 25 cycles of 2) denaturation (94 °C for 30 s), annealing (57 °C for 30 s), and extension (72 °C for 30 s), and 3) final extension step at 72 °C for 5 min.

### 2.4. Sequencing and sequence processing

Samples were sequenced at Celemics (Seoul, Korea), with Illumina HiSeq2000 platform. Raw fastq sequence files were submitted to Sequence Read Archive (SRA) with the accession number SRP049281. Adaptor sequences with 2 base-pairs in length were removed using Trimmomatic (Bolger et al., 2014) and paired end sequences were combined together with PANDAseq (Masella et al., 2012). PANDAseq sequence quality control threshold was set as 9 and minimum overlap between two sequences were set as 4.

Downstream analysis was performed with Mothur (Schloss

et al., 2009). Sequences with bad quality, for example, sequences with large ambiguity and sequences with short read length, and chimeric sequences were removed. SILVA 119 database (Quast et al., 2012) was used for alignment and Eztaxon database (Chun et al., 2007) was used for classification of bacterial sequences. Sequences with more than 97% similarity was combined as an operational taxonomic unit (OTU) and singletons were removed. Detailed commend line is provided in APPENDIX.

For functional analysis, sequence processing were performed by SILVAngs, a data analysis service online (URL: <https://www.arb-silva.de/ngs/>). Default options were used except for: 1) similarity threshold used for creating OTUs (default: 0.98, manual: 0.97), 2) classification similarity (default: 0.93, manual: 0.97), 3) SILVA database release version (default: 123, manual: 119.1), and 4) minimum length of sequence to filter (default: 50, manual: 150).

## 2.5. Statistical analysis

To do OTU-based analysis, sequences from each group were subsampled to the equal number of sequences. Compositional difference of bacterial community between magnetically-enriched and magnetically-depleted fraction was computed by analysis of similarity (ANOSIM) and multi-response permutation procedure (MRPP) with 999 permutation. For the analyses, read numbers of each OTU were square-root transformed and distance between

samples was calculated based on bray–curtis distance. To visualize the difference between two groups, non–metric multidimensional scaling (nMDS) plot based on the dissimilarity was generated using R software ver. 3.2.2.

Other analyses or figure generation were also done by using R, including indicator species analysis, functional analysis, rarefaction curve generation, and heatmap generation. Indicator species values of top 100 OTUs were calculated by using “labdsv” R package. For functional analysis, newly developed R package “Tax4Fun” was used (Aßhauer et al., 2015). Tax4Fun is a tool used for the prediction of metabolic and functional profiles based on taxonomic data. As an input, the file generated from SILVAngs was used.

## **2.6. Structural and microstructural configuration of magnetically–enriched fraction**

To validate whether the magnetically–enriched fraction was composed mostly of magnetite, additional samples were collected. Samples were subjected to magnetic separation and the black magnetic mineral was washed with 95% alcohol several times for the purpose of the removal of organic matters that might hinder the observation of crystallography. The structural characterization of the mineral was performed in Mechanical and Aerospace Engineering laboratory, Seoul National University, Korea. The gross structure of magnetically–enriched fraction was evaluated by

X-ray diffraction (XRD, D8 advance by DAVINCI) (CuK $\alpha$  radiation was used) with  $2\theta$  in the range of 10–80°, step scanned with scanning speed of 0.02° per min. For the detailed structural and microstructural characterization of the crystal, high resolution TEM (HRTEM) (JEOL–2100) was used. To observe the mode of growth and the variation of surface morphology, scanning ion microscope (SIM) imaging (CORBRA–FIB, Orsay physics) was used with 23 pA of beam current. For cross sectional imaging, the focused ion beam (FIM) was used with 2.5 nA and 139 pA of beam current and 45° tilted images were taken.

## 2.7. Quantitative PCR analysis

To measure bacterial 16S rRNA gene copy number of magnetically–enriched fraction compared to bulk sediment, additional 4 point samples were taken from the pond. Some portion of each sediment samples was kept as bulk sediment, and the others were subjected to magnetic separation. The same soil extraction kit described above was used with 0.5 g of soil from each sample.

The quantitative PCR (qPCR) analysis was performed at Ecological Engineering laboratory, School of Civil and Environmental Engineering, Yonsei University, Korea. For each sample, the total mixture volume was 20  $\mu\text{l}$  including specific bacterial primer, 341 F (5' –CCTACGGGAGGCAGCAG–3' ) and 797 R (5' –GGACTACCAGGGTCTAATCCTGTT–3' ). CFX96 machine (Bio–Rad, USA) and SYBR Green dye (Bio–Rad, USA)

was used for detection. PCR condition was as follows: 44 cycles of 1) denaturation step at 94 °C for 25 s, 2) annealing step at 64.5 °C for 25 s, and 3) extension step at 72 °C for 25 s. For each sample, qPCR analysis was performed twice to increase the reliability. 10-fold dilution series of plasmids that contain the bacterial 16S rRNA gene from environmental samples were used to create standard curve. Significance between bulk soil and magnetically-enriched fraction was tested by using Wilcoxon rank sum test which is a non-parametric test of t-test.

## 3. Result

### 3.1. Presence and Microstructure of Magnetite in the magnetically-enriched fraction

The typical XRD pattern of magnetically-enriched fraction is shown in Fig. 3. The identities of the peaks match with the spinal structures of magnetite ( $\text{Fe}_3\text{O}_4$ -JCPDS-04-005-4551) and maghemite ( $\gamma$   $\text{Fe}_2\text{O}_3$ -JCPDS-3901346) and hematite ( $\text{Fe}_2\text{O}_3$ -JCPDS-01-079-1741), a trigonal form of iron oxide. The result of a comparative analysis of maximum intensity peaks indicates magnetite as the dominant species (75%) followed by hematite at substantially lower concentrations (25%). Additionally, a small fraction of maghemite can be attributed to the surface oxidation of the magnetite.

Furthermore, the surface microstructure of the material extracted magnetically from the sediment was characterized by scanning ion microscopy (SIM), shown in Fig. 4(a). Fig. 4(a). This revealed an abundance of particles exhibiting spiral growth with triangular morphology and well faceted steps. The triangular morphology is indicative of the epitaxial growth of large particles along the (111) direction as in the case of magnetite polyhedron (Su et al., 2012). Further, in order to confirm the difference between the two spiral steps, the grain was drilled using focused ion beam (FIB). The selected section (encircled) shown in Fig. 4(b) was cut by FIB and the interior cross sectional image (inset of Fig.

4(b)–Fig. 4(e)) indicates the co-existence of multi-structures between the two steps which might possibly arise from the structural defect occurring during the formation of spiral steps. Furthermore this observation has also been confirmed by high resolution TEM (HRTEM). The bright field micrograph (Fig. 4(c)) of the pond sediments shows the presence of lattice fringes. The Fast Fourier Transform (FFT) in Fig. 4(d) originates from the square region of Fig. 4(b). The FFT shows the presence of (111) types of crystallographic planes of magnetite with lattice parameters  $a=b=c=8.40\text{\AA}$ . Surface topography along with the crystallographic observation confirms the presence of magnetite in the pond sediment. Given this mineralogical evidence of magnetite, from this point onwards in this thesis the magnetically-enriched fraction will be referred to as ‘magnetite-enriched’ group, and magnetically depleted fraction will be referred to as ‘magnetite-depleted’ group.

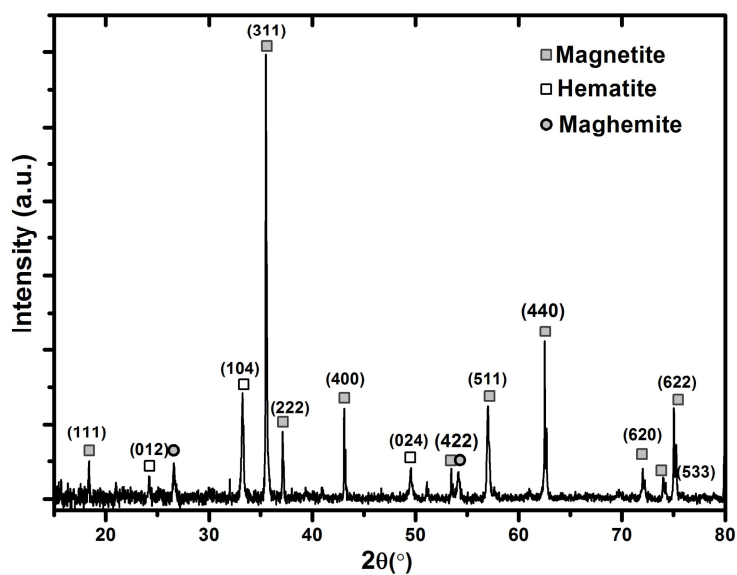


**Fig. 3** Typical XRD pattern observed for pond sediment showing the presence of magnetite and hematite phase in pond sediment. A small fraction of oxidized form of magnetite and maghemite is also visible possibly due to surface oxidation of magnetite during the washing of sediment by ethanol

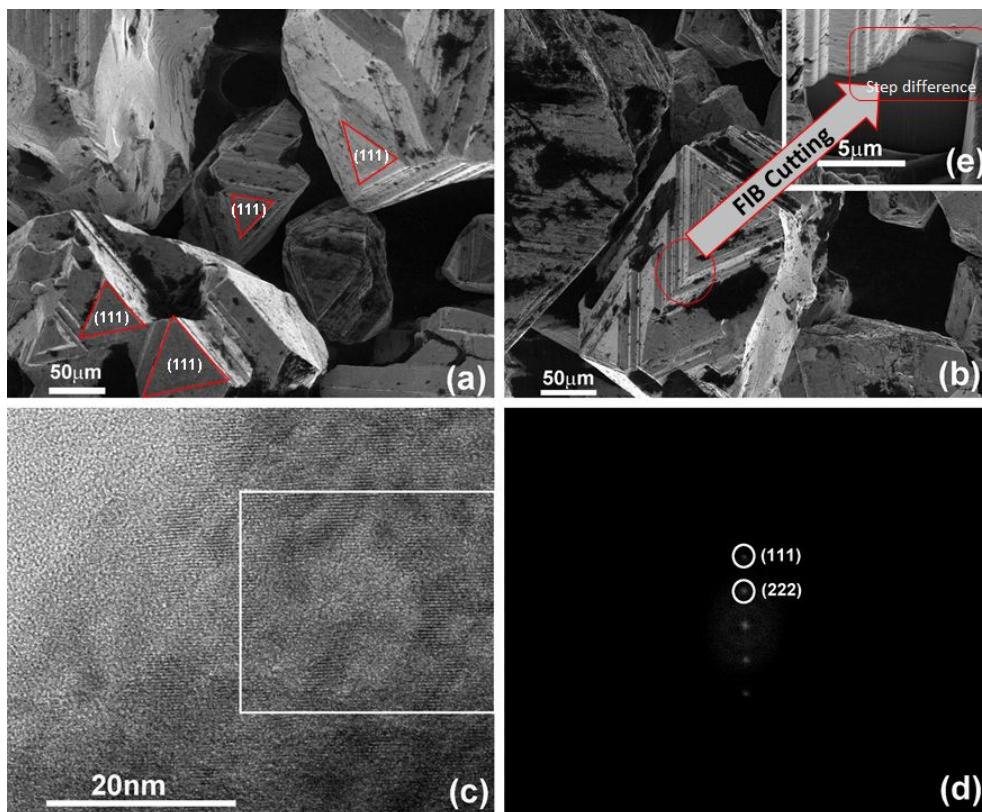


**Fig. 4** Scanning ion micrographic image of sediment a indicating the spiral step growth along (111) crystallographic direction as suggested by the triangular morphology. b The encircled section subject to FIB cross-section cutting is shown in the inset Fig (e) indicative the presence of defects between the two steps. c The HRTEM micrograph showing the lattice presence typical of a crystal structure. d FFT of square section of c indicating the stacking of (111) type planes

### 3.2. Bacterial community structure of magnetite-enriched fraction

The total number of bacterial sequences obtained from 8 samples (4 magnetite depleted, 4 magnetite enriched) was 246,678 ranging from 5,249 to 39,809 per sample. In both the magnetite-depleted and magnetite-enriched groups, Proteobacteria was dominant, followed by Bacteroidetes (magnetite-depleted group) and Acidobacteria (magnetite-enriched group) (Fig. 5). Species accumulation rate of each group is shown in Fig. 6. The magnetite-enriched group had relatively higher species accumulation rate compared to magnetite-depleted group and had relatively uniform trend in all 4 samples (Fig. 6).

In terms of overall bacterial community structure, the magnetite-depleted and magnetite-enriched group were distinct from each other as shown in the ordination (Fig. 7) and the result of ANOSIM ( $R=0.8958$ ,  $p=0.03$ ) and MRPP ( $A=0.1111$ ,  $p=0.035$ ). The heatmap of the relative abundance of the top 50 OTUs also shows the substantial difference between two groups in OTU level (Fig. 8). The most abundant OTU in the magnetite-enriched group (OTU5) was a member of the genus *Geobacter*, which is already known from laboratory experiments to include several magnetite formers. OTU5 was designated as an indicator species (indicator value=0.94428,  $p=0.025$ ) of magnetite-enriched group according to indicator species analysis result (Table 2). As presented in Table 2, indicator species (among top 500 OTUs) of each group

belonged to several different phylum and class, having no consistent phylogenetic lineages.

The bacterial community functional analysis result, predicted based on taxonomic information by using “Tax4Fun” R package, shows that in both two groups, house-keeping genes, for example, genes related to two-component system and ABC transporters, were most abundant (Table A1). All of the most abundant 50 functions showed not much difference in their relative abundance between two groups, while the average relative abundance of magnetite-enriched group divided by that of magnetite-depleted group ranged from 0.91 to 1.18.

Bacterial 16S rRNA copy number (log<sub>10</sub>-transformed) was not significantly different ( $p=1$ ) between bulk sediment and magnetite-enriched group based on qPCR result (Fig. 9).

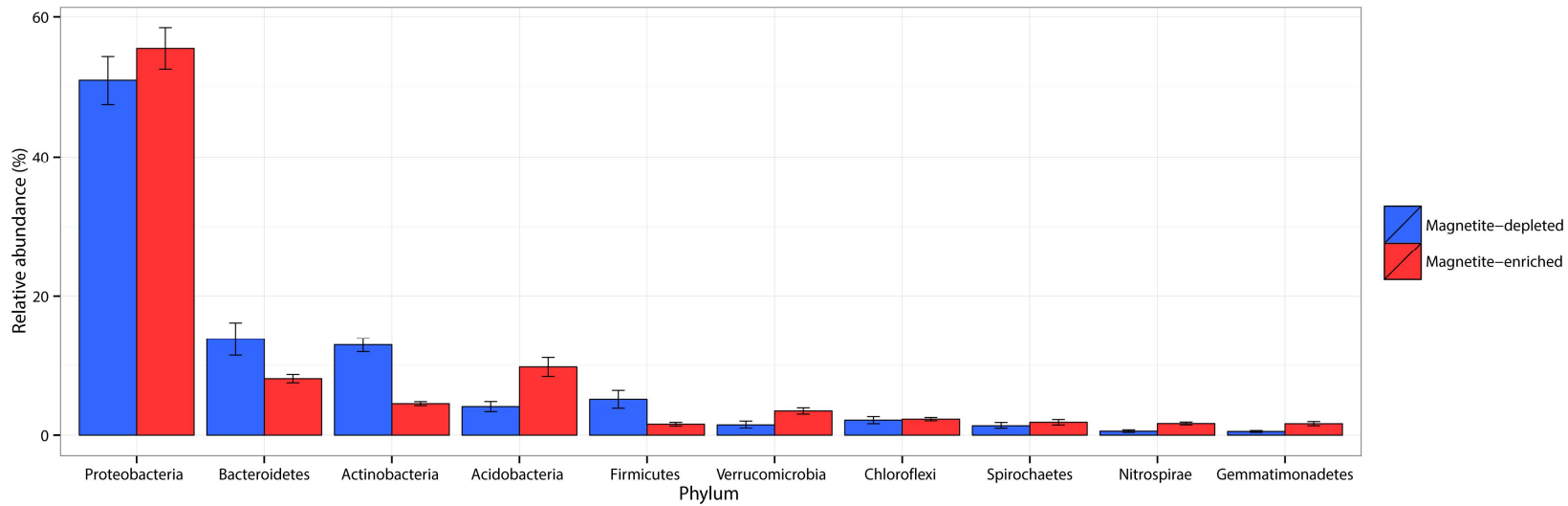


**Fig. 5** Phylum breakdown of magnetite-enriched and magnetite-depleted group

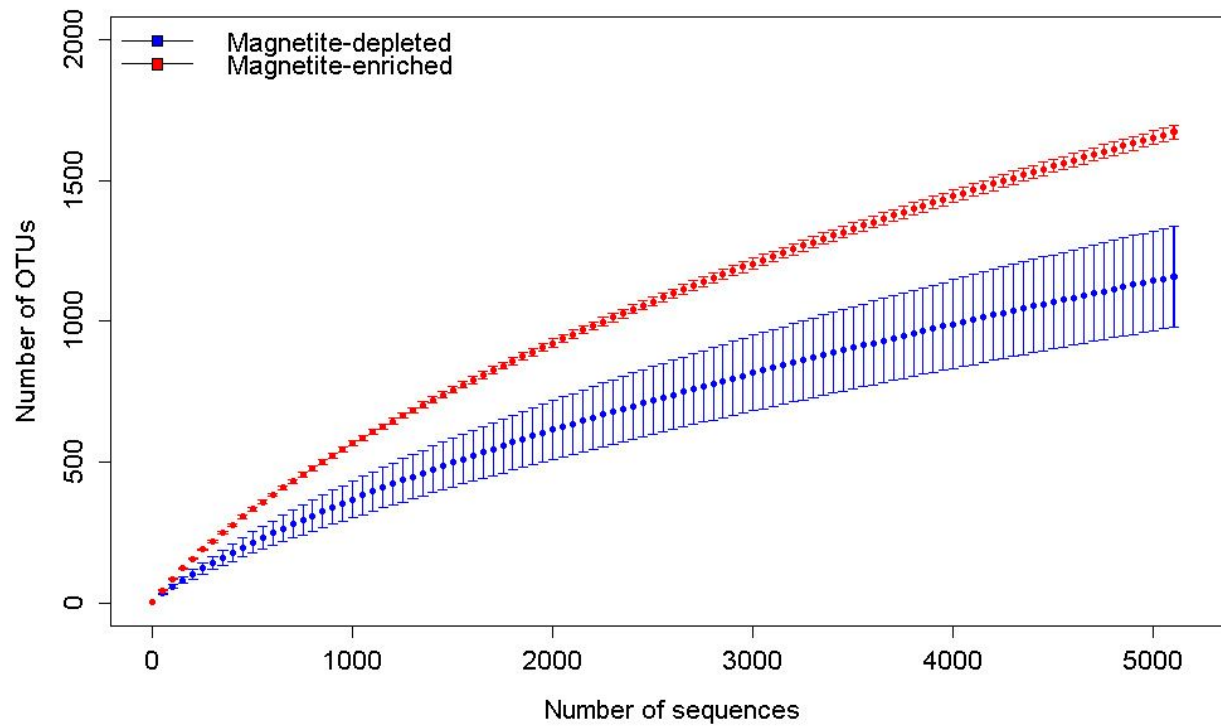
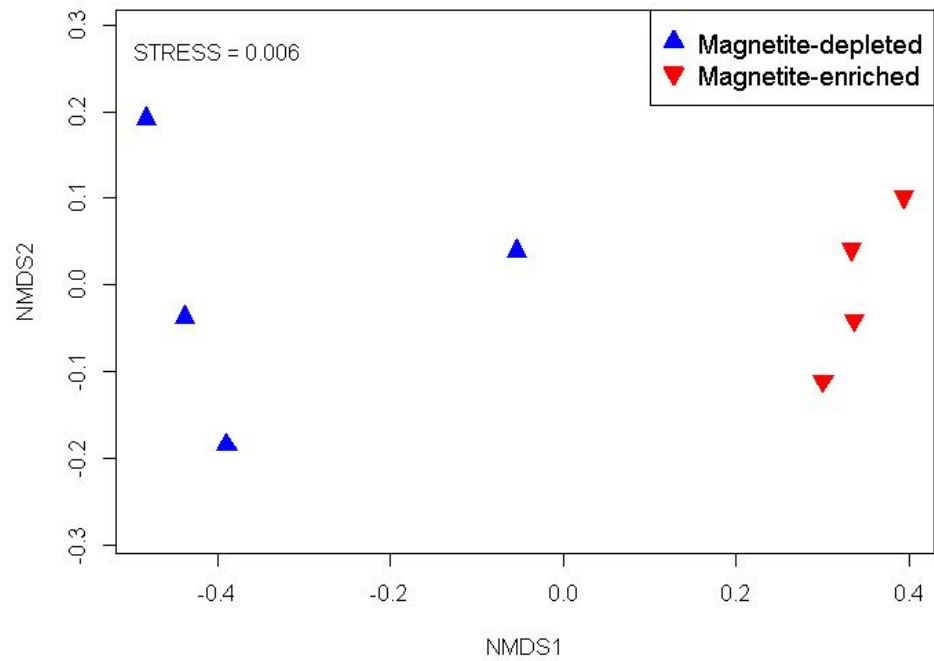


Fig. 6 Rarefaction curve showing species accumulation rate of magnetite-enriched and magnetite-depleted group



**Fig. 7** nMDS plot showing taxonomic distance between each sample

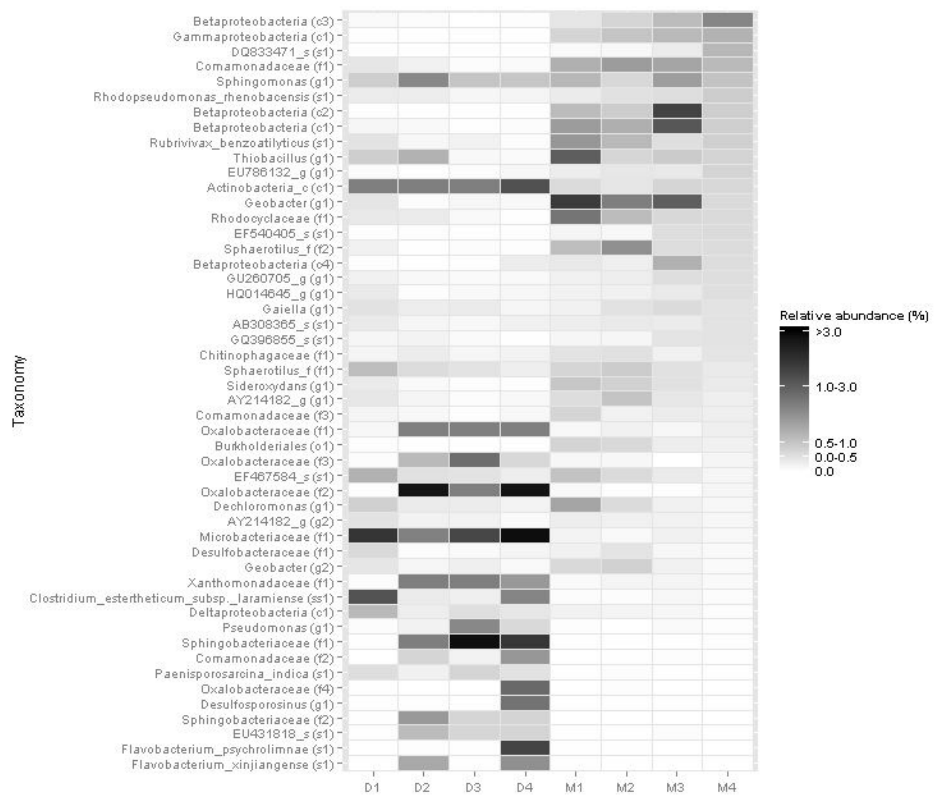
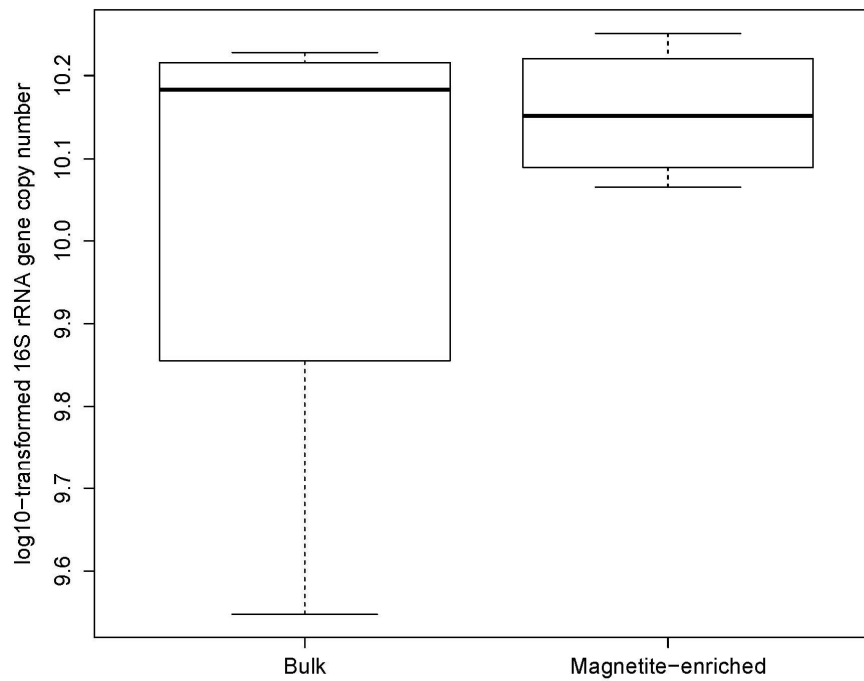


Fig. 8 Heatmap showing the relative abundance of the 50 most abundant OTUs



**Fig. 9** qPCR result for 16S gene copy number (a measure of bacterial cell abundance) of bulk sediment group and magnetite-enriched group

**Table 2** Indicator species of magnetite–depleted (D) and magnetite–enriched (M) group among top 500 OTUs

OTU	D (%)	M (%)	M/D	GROUP	INDICATOR VALUE	P-VALUE	TAXONOMY (PHYLUM, CLASS, ORDER, FAMILY, GENUS, SPECIES, SUBSPECIES)
OTU2	5.895	0.617	0.10	D	0.91	0.033	<i>Actinobacteria, Actinobacteria_c, unclassified, unclassified, unclassified, unclassified, unclassified, unclassified</i>
OTU4	3.631	0.167	0.05	D	0.96	0.028	<i>Actinobacteria, Actinobacteria_c, Micrococcales, Microbacteriaceae, unclassified, unclassified, unclassified</i>
OTU5	0.186	3.156	16.95	M	0.94	0.025	<i>Proteobacteria, Deltaproteobacteria, Desulfuromonadales, Geobacteraceae, Geobacter, unclassified, unclassified</i>
OTU9	1.524	0.078	0.05	D	0.95	0.025	<i>Firmicutes, Clostridia, Clostridiales, Clostridiaceae, Clostridium, Clostridium_estertheticum, Clostridium_estertheticum_subsp._laramiense</i>
OTU11	0.206	1.504	7.31	M	0.88	0.027	<i>Proteobacteria, Betaproteobacteria, Burkholderiales, Comamonadaceae, unclassified, unclassified, unclassified</i>
OTU12	0.083	1.803	21.65	M	0.96	0.031	<i>Proteobacteria, Betaproteobacteria, unclassified, unclassified, unclassified, unclassified, unclassified</i>
OTU13	0.005	1.627	332.00	M	1.00	0.034	<i>Proteobacteria, Betaproteobacteria, unclassified, unclassified, unclassified, unclassified, unclassified</i>
OTU14	0.216	1.259	5.84	M	0.85	0.036	<i>Proteobacteria, Betaproteobacteria, Rhodocyclales, Rhodocyclaceae, unclassified, unclassified, unclassified</i>
OTU16	0.225	1.127	5.00	M	0.83	0.026	<i>Proteobacteria, Betaproteobacteria, Burkholderiales,</i>

							<i>Sphaerotilus_f, Rubrivivax, Rubrivivax_benzoatilyticus, unclassified</i>
OTU17	0.044	1.132	25.67	M	0.96	0.034	<i>Proteobacteria, Betaproteobacteria, unclassified, unclassified, unclassified, unclassified</i>
OTU18	0.088	1.093	12.39	M	0.93	0.031	<i>Proteobacteria, Betaproteobacteria, Burkholderiales, Sphaerotilus_f, unclassified, unclassified, unclassified</i>
OTU23	0.005	1.083	221.00	M	1.00	0.022	<i>Proteobacteria, Gammaproteobacteria, unclassified, unclassified, unclassified, unclassified</i>
OTU25	0.123	0.666	5.44	M	0.84	0.048	<i>Proteobacteria, Betaproteobacteria, Gallionellales, Gallionellaceae, Sideroxydans, unclassified, unclassified</i>
OTU26	0.627	0.142	0.23	D	0.82	0.035	<i>Proteobacteria, Deltaproteobacteria, unclassified, unclassified, unclassified, unclassified</i>
OTU27	0.245	0.583	2.38	M	0.70	0.025	<i>Proteobacteria, Alphaproteobacteria, Rhizobiales, Bradyrhizobiaceae, Rhodopseudomonas, Rhodopseudomonas_rhenobacensis, unclassified</i>
OTU37	0.838	0.000	0.00	D	1.00	0.027	<i>Bacteroidetes, Sphingobacteria, Sphingobacteriales, Sphingobacteriaceae, unclassified, unclassified, unclassified</i>
OTU39	0.519	0.015	0.03	D	0.97	0.032	<i>Firmicutes, Bacilli, Bacillales, Planococcaceae, Paenisporosarcina, Paenisporosarcina_indica, unclassified</i>
OTU41	0.015	0.490	33.33	M	0.97	0.041	<i>Proteobacteria, Betaproteobacteria, Burkholderiales, unclassified, unclassified, unclassified, unclassified</i>
OTU44	0.108	0.387	3.59	M	0.78	0.02	<i>Proteobacteria, Betaproteobacteria, Burkholderiales, Comamonadaceae, unclassified, unclassified, unclassified</i>

OTU47	0.000	0.451	–	M	1.00	0.026	<i>Proteobacteria, Gammaproteobacteria, FN820314_o, DQ833471_f, DQ833471_g, DQ833471_s, unclassified</i>
OTU48	0.059	0.470	8.00	M	0.89	0.02	<i>Proteobacteria, Betaproteobacteria, EU786132_o, EU786132_f, EU786132_g, unclassified, unclassified</i>
OTU49	0.025	0.372	15.20	M	0.94	0.038	<i>Proteobacteria, Gammaproteobacteria, Chromatiales, Acidiferrobacter_f, Acidiferrobacter, EF540405_s, unclassified</i>
OTU52	0.074	0.314	4.27	M	0.81	0.034	<i>Bacteroidetes, Bacteroidia, Bacteroidales, GU454901_f, GU454901_g, unclassified, unclassified</i>
OTU55	0.000	0.377	–	M	1.00	0.034	<i>Acidobacteria, Holophagae, Holophagales, Holophagaceae, unclassified, unclassified, unclassified</i>
OTU62	0.000	0.402	–	M	1.00	0.026	<i>Proteobacteria, Betaproteobacteria, Gallionellales, Gallionellaceae, Gallionella, CP002159_s, unclassified</i>
OTU65	0.235	0.108	0.46	D	0.69	0.024	<i>Bacteroidetes, Flavobacteria, Flavobacteriales, Flavobacteriaceae, Flavobacterium, EU662323_s, unclassified</i>
OTU68	0.054	0.260	4.82	M	0.83	0.038	<i>Acidobacteria, Chloracidobacterium_c, Blastocatella_o, AY281358_f, AY281358_g, unclassified, unclassified</i>
OTU71	0.010	0.279	28.50	M	0.97	0.025	<i>Proteobacteria, Betaproteobacteria, Gallionellales, Gallionellaceae, Gallionella, unclassified, unclassified</i>
OTU76	0.059	0.221	3.75	M	0.79	0.025	<i>Bacteroidetes, Bacteroidia, Bacteroidales, GU454901_f, GQ396981_g, GQ396981_s, unclassified</i>
OTU77	0.059	0.225	3.83	M	0.79	0.024	<i>Acidobacteria, Chloracidobacterium_c, Blastocatella_o, AY281358_f, AY281358_g, unclassified, unclassified</i>

OTU78	0.044	0.245	5.56	M	0.85	0.026	<i>Nitrospirae, Nitrospira_c, Nitrospirales, Nitrospiraceae, Nitrospira, DQ058676_s, unclassified</i>
OTU79	0.064	0.255	4.00	M	0.80	0.021	<i>Nitrospirae, GU444092_c, GU444092_o, GU444092_f, GU444092_g, unclassified, unclassified</i>
OTU88	0.010	0.191	19.50	M	0.95	0.026	<i>Proteobacteria, Gammaproteobacteria, Chromatiales, Acidiferrobacter_f, Acidiferrobacter, EU266783_s, unclassified</i>
OTU91	0.020	0.211	10.75	M	0.91	0.027	<i>Proteobacteria, Deltaproteobacteria, FM253572_o, EU491430_f, JF718671_g, unclassified, unclassified</i>
OTU99	0.029	0.196	6.67	M	0.87	0.024	<i>Acidobacteria, EU686603_c, EU686603_o, EU686603_f, HQ190410_g, unclassified, unclassified</i>
OTU102	0.029	0.176	6.00	M	0.86	0.028	<i>Gemmatimonadetes, Gemmatimonadetes_c, Gemmatimonadales, EU881211_f, EU881211_g, unclassified, unclassified</i>
OTU104	0.005	0.206	42.00	M	0.98	0.034	<i>Proteobacteria, Betaproteobacteria, Sterolibacterium_o, Sterolibacterium_f, AB186832_g, unclassified, unclassified</i>
OTU107	0.010	0.201	20.50	M	0.95	0.02	<i>Proteobacteria, Deltaproteobacteria, Desulfobulbaceae_o, Desulfurivibrio_f, EU016437_g, EU016437_s, unclassified</i>
OTU109	0.005	0.230	47.00	M	0.98	0.036	<i>Proteobacteria, Betaproteobacteria, unclassified, unclassified, unclassified, unclassified</i>
OTU114	0.010	0.225	23.00	M	0.96	0.021	<i>Proteobacteria, Gammaproteobacteria, unclassified, unclassified, unclassified, unclassified</i>
OTU119	0.000	0.186	–	M	1.00	0.034	<i>Proteobacteria, Betaproteobacteria, unclassified, unclassified, unclassified, unclassified</i>

OTU124	0.015	0.191	13.00	M	0.93	0.033	<i>Gemmatimonadetes, Gemmatimonadetes_c, Gemmatimonadales, Gemmatimonadaceae, EU421850_g, EU421850_s, unclassified</i>
OTU131	0.010	0.201	20.50	M	0.95	0.033	<i>Proteobacteria, Deltaproteobacteria, unclassified, unclassified, unclassified, unclassified</i>
OTU134	0.083	0.201	2.41	M	0.71	0.03	<i>Actinobacteria, Rubrobacteria, Gaiellales, Gaiellaceae, Gaiella, unclassified, unclassified</i>
OTU136	0.005	0.225	46.00	M	0.98	0.03	<i>Verrucomicrobia, Verrucomicrobiae, Verrucomicrobiales, Chthoniobacter_f, Chthoniobacter, unclassified, unclassified</i>
OTU137	0.010	0.196	20.00	M	0.95	0.038	<i>Proteobacteria, Deltaproteobacteria, Myxococcales, Polyangiaceae, JF719608_g, unclassified, unclassified</i>
OTU145	0.069	0.162	2.36	M	0.70	0.04	<i>Acidobacteria, EU686603_c, EU686603_o, EU686603_f, EU861837_g, AF013534_s, unclassified</i>
OTU153	0.225	0.000	0.00	D	1.00	0.035	<i>Actinobacteria, Actinobacteria_c, unclassified, unclassified, unclassified, unclassified, unclassified</i>
OTU155	0.039	0.137	3.50	M	0.78	0.027	<i>Proteobacteria, Betaproteobacteria, Burkholderiales, AY234747_f, AY234747_g, GQ396821_s, unclassified</i>
OTU163	0.025	0.157	6.40	M	0.86	0.026	<i>Proteobacteria, Alphaproteobacteria, Rhodospirillales, FM209092_f, DQ451508_g, AY913269_s, unclassified</i>
OTU177	0.015	0.123	8.33	M	0.89	0.033	<i>Proteobacteria, Gammaproteobacteria, Steroidobacter_o, DQ984612_f, DQ984612_g, DQ984612_s, unclassified</i>
OTU183	0.015	0.108	7.33	M	0.88	0.025	<i>Proteobacteria, Betaproteobacteria, DQ009366_o, AM990454_f, GQ263935_g, unclassified, unclassified</i>

OTU186	0.010	0.137	14.00	M	0.93	0.024	<i>Acidobacteria, Holophagae, Holophagales, Holophagaceae, Holophaga, unclassified, unclassified</i>
OTU187	0.000	0.142	–	M	1.00	0.035	<i>Acidobacteria, Holophagae, Holophagales, Holophagaceae, Holophaga, unclassified, unclassified</i>
OTU194	0.039	0.123	3.13	M	0.76	0.035	<i>Actinobacteria, Thermoleophilia, Solirubrobacterales, AB630582_f, AB630582_g, unclassified, unclassified</i>
OTU197	0.015	0.142	9.67	M	0.91	0.026	<i>Gemmatimonadetes, Gemmatimonadetes_c, Gemmatimonadales, EU881211_f, unclassified, unclassified, unclassified</i>
OTU202	0.029	0.152	5.17	M	0.84	0.035	<i>Nitrospirae, Nitrospira_c, Nitrospirales, Nitrospiraceae, Nitrospira, AB252940_s, unclassified</i>
OTU204	0.010	0.132	13.50	M	0.93	0.029	<i>Proteobacteria, Deltaproteobacteria, unclassified, unclassified, unclassified, unclassified</i>
OTU208	0.000	0.147	–	M	1.00	0.019	<i>Proteobacteria, Betaproteobacteria, Methylophilales, Methylophilaceae, unclassified, unclassified, unclassified</i>
OTU214	0.000	0.172	–	M	1.00	0.026	<i>Proteobacteria, Betaproteobacteria, Burkholderiales, Alcaligenaceae, unclassified, unclassified, unclassified</i>
OTU215	0.020	0.127	6.50	M	0.87	0.026	<i>Gemmatimonadetes, Gemmatimonadetes_c, Gemmatimonadales, EU881211_f, EU881211_g, EU881211_s, unclassified</i>
OTU222	0.000	0.088	–	M	1.00	0.037	<i>Proteobacteria, Gammaproteobacteria, Xanthomonadales, Xanthomonadaceae, unclassified, unclassified, unclassified</i>
OTU227	0.000	0.127	–	M	1.00	0.027	<i>Proteobacteria, Betaproteobacteria, Gallionellales, Gallionellaceae, unclassified, unclassified, unclassified</i>

OTU230	0.010	0.137	14.00	M	0.93	0.029	<i>Proteobacteria, Betaproteobacteria, Methylophilales, Methylophilaceae, Sulfuricella, unclassified, unclassified</i>
OTU231	0.015	0.123	8.33	M	0.89	0.032	<i>Acidobacteria, EU686603_c, EU686603_o, EU686603_f, HQ190410_g, unclassified, unclassified</i>
OTU235	0.137	0.039	0.29	D	0.78	0.033	<i>Actinobacteria, Actinobacteria_c, Propionibacteriales, Nocardioideae, Nocardioides, AB240337_s, unclassified</i>
OTU238	0.088	0.010	0.11	D	0.90	0.034	<i>Actinobacteria, Rubrobacteria, AB240334_o, EU407208_f, EU407208_g, EU407208_s, unclassified</i>
OTU247	0.000	0.098	–	M	1.00	0.034	<i>Bacteroidetes, Bacteroidia, Bacteroidales, Prolixibacter_f, AB240481_g, GU112203_s, unclassified</i>
OTU248	0.000	0.093	–	M	1.00	0.015	<i>Spirochaetes, Spirochaetes_c, Spirochaetales, Spirochaetaceae, AY214182_g, unclassified, unclassified</i>
OTU260	0.010	0.098	10.00	M	0.91	0.034	<i>Proteobacteria, Deltaproteobacteria, Myxococcales, Polyangiaceae, unclassified, unclassified, unclassified</i>
OTU267	0.005	0.098	20.00	M	0.95	0.028	<i>Gemmatimonadetes, Gemmatimonadetes_c, Gemmatimonadales, Gemmatimonadaceae, unclassified, unclassified, unclassified</i>
OTU268	0.000	0.088	–	M	1.00	0.023	<i>Bacteroidetes, unclassified, unclassified, unclassified, unclassified, unclassified, unclassified</i>
OTU269	0.025	0.098	4.00	M	0.80	0.027	<i>Actinobacteria, Actinobacteria_c, Planktophila_o, Planktophila_f, Planktophila, EU117782_s, unclassified</i>
OTU270	0.010	0.103	10.50	M	0.91	0.036	<i>Nitrospirae, GU444092_c, GU444092_o, GU444092_f, GU444092_g, unclassified, unclassified</i>

OTU271	0.015	0.103	7.00	M	0.88	0.032	<i>Acidobacteria, EU686603_c, EU686603_o, EU686603_f, HQ864177_g, unclassified, unclassified</i>
OTU272	0.049	0.118	2.40	M	0.71	0.034	<i>Proteobacteria, Betaproteobacteria, Burkholderiales, AY234747_f, AY234747_g, EU335273_s, unclassified</i>
OTU281	0.020	0.098	5.00	M	0.83	0.025	<i>Proteobacteria, Deltaproteobacteria, Desulfarculales, Desulfarculaceae, unclassified, unclassified, unclassified</i>
OTU284	0.005	0.108	22.00	M	0.96	0.029	<i>Acidobacteria, Holophagae, Holophagales, Holophagaceae, Holophaga, unclassified, unclassified</i>
OTU292	0.000	0.093	–	M	1.00	0.037	<i>Proteobacteria, Betaproteobacteria, unclassified, unclassified, unclassified, unclassified</i>
OTU304	0.078	0.015	0.19	D	0.84	0.019	<i>Proteobacteria, Gammaproteobacteria, Methylococcales, Methylomonas_f, unclassified, unclassified, unclassified</i>
OTU309	0.078	0.025	0.31	D	0.76	0.032	<i>Acidobacteria, EU686603_c, EU686603_o, EU686603_f, unclassified, unclassified, unclassified</i>
OTU310	0.025	0.098	4.00	M	0.80	0.036	<i>Acidobacteria, EU686603_c, EU686603_o, EU686603_f, GU187031_g, unclassified, unclassified</i>
OTU315	0.010	0.074	7.50	M	0.88	0.028	<i>Proteobacteria, Deltaproteobacteria, FM253572_o, EU491430_f, JF718671_g, unclassified, unclassified</i>
OTU318	0.000	0.093	–	M	1.00	0.035	<i>Chlorobi, Ignavibacteriae, Ignavibacteriales, GQ472436_f, AY221073_g, unclassified, unclassified</i>
OTU324	0.093	0.010	0.11	D	0.90	0.029	<i>Actinobacteria, Rubrobacteria, AB240334_o, EU407208_f, EU407208_g, unclassified, unclassified</i>
OTU330	0.015	0.098	6.67	M	0.87	0.048	<i>Proteobacteria, Betaproteobacteria, Burkholderiales, Sphaerotilus_f, unclassified, unclassified, unclassified</i>

OTU332	0.000	0.093	–	M	1.00	0.026	<i>Proteobacteria, Betaproteobacteria, Zoogloea_o, Zoogloea_f, Azoarcus, unclassified, unclassified</i>
OTU338	0.000	0.083	–	M	1.00	0.026	<i>Firmicutes, Clostridia, Clostridiales, Veillonellaceae, Megasphaera, DQ278866_s, unclassified</i>
OTU353	0.015	0.098	6.67	M	0.87	0.034	<i>Proteobacteria, Betaproteobacteria, EU786132_o, EU786132_f, EU786132_g, unclassified, unclassified</i>
OTU358	0.000	0.088	–	M	1.00	0.022	<i>Bacteroidetes, Cytophagia, Cytophagales, Cytophagaceae, Arcicella, AJ290033_s, unclassified</i>
OTU372	0.034	0.000	0.00	D	1.00	0.026	<i>Proteobacteria, Gammaproteobacteria, Methylococcales, Methylomonas_f, unclassified, unclassified, unclassified</i>
OTU373	0.000	0.074	–	M	1.00	0.029	<i>Bacteroidetes, Flavobacteria, Flavobacteriales, Brumimicrobiaceae, Fluvicola, AF289153_s, unclassified</i>
OTU378	0.010	0.069	7.00	M	0.88	0.036	<i>Acidobacteria, EU686603_c, EU686603_o, EU686603_f, HQ190410_g, unclassified, unclassified</i>
OTU396	0.113	0.000	0.00	D	1.00	0.022	<i>Bacteroidetes, Sphingobacteria, Sphingobacteriales, Chitinophagaceae, unclassified, unclassified, unclassified</i>
OTU404	0.005	0.054	11.00	M	0.92	0.033	<i>Nitrospirae, GU444092_c, GU444092_o, GU444092_f, GU444092_g, unclassified, unclassified</i>
OTU408	0.000	0.083	–	M	1.00	0.028	<i>Proteobacteria, Betaproteobacteria, Burkholderiales, Comamonadaceae, Limnohabitans, unclassified, unclassified</i>
OTU409	0.015	0.054	3.67	M	0.79	0.031	<i>Acidobacteria, EU686603_c, EU686603_o, EU686603_f, GU260705_g, unclassified, unclassified</i>
OTU413	0.010	0.059	6.00	M	0.86	0.028	<i>Bacteroidetes, Bacteroidia, Bacteroidales, Prolixibacter_f, HQ178936_g, DQ404739_s, unclassified</i>

OTU424	0.000	0.074	–	M	1.00	0.03	<i>Proteobacteria, Gammaproteobacteria, unclassified, unclassified, unclassified, unclassified, unclassified</i>
OTU427	0.000	0.074	–	M	1.00	0.027	<i>Acidobacteria, Holophagae, Holophagales, Holophagaceae, Holophaga, unclassified, unclassified</i>
OTU429	0.005	0.054	11.00	M	0.92	0.021	<i>Acidobacteria, Chloracidobacterium_c, Blastocatella_o, AY281358_f, AY281358_g, HQ864078_s, unclassified</i>
OTU435	0.005	0.078	16.00	M	0.94	0.027	<i>Bacteroidetes, Bacteroidia, Bacteroidales, Prolixibacter_f, HQ178936_g, unclassified, unclassified</i>
OTU453	0.005	0.064	13.00	M	0.93	0.05	<i>Proteobacteria, Deltaproteobacteria, unclassified, unclassified, unclassified, unclassified</i>
OTU458	0.000	0.064	–	M	1.00	0.026	<i>Bacteroidetes, Bacteroidia, Bacteroidales, Prolixibacter_f, AJ229237_g, EF562567_s, unclassified</i>
OTU462	0.000	0.044	–	M	1.00	0.034	<i>Nitrospirae, GU444092_c, GU444092_o, DQ906831_f, DQ906831_g, EU881155_s, unclassified</i>
OTU463	0.049	0.005	0.10	D	0.91	0.031	<i>Acidobacteria, EU686603_c, EU686603_o, EU686603_f, GU187031_g, DQ648904_s, unclassified</i>
OTU474	0.010	0.044	4.50	M	0.82	0.031	<i>Verrucomicrobia, Verrucomicrobiae, Pedosphaera_o, Pedosphaera_f, Pedosphaera, unclassified, unclassified</i>
OTU482	0.044	0.000	0.00	D	1.00	0.025	<i>Proteobacteria, Deltaproteobacteria, unclassified, unclassified, unclassified, unclassified</i>
OTU483	0.000	0.049	–	M	1.00	0.024	<i>Proteobacteria, Alphaproteobacteria, Rhizobiales, unclassified, unclassified, unclassified, unclassified</i>
OTU496	0.015	0.069	4.67	M	0.82	0.04	<i>Proteobacteria, Betaproteobacteria, AB308366_o, HQ014645_f, HQ014645_g, unclassified, unclassified</i>

## 4. Discussion

### 4.1. Greater relative abundance of *Geobacter* in magnetite–enriched group

The greater relative abundance of *Geobacter* in the magnetite–enriched samples is suggestive of their role in natural habitats in the process of magnetite formation, something that has only been investigated in laboratory culture conditions. *Geobacter* was the first organism known to obtain energy through dissimilatory iron reduction (Lovley et al., 1987). In culture condition, where nutrient source is provided, several species who belongs to *Geobacter* are able to form magnetite through iron reduction. Their ability to couple organic matter oxidation with iron reduction has been studied and applied to several different fields, for example, in biotechnology, they are used for the purpose of bioremediation of organic or metal contaminated area (Amos et al., 2007). Also, their ability to transfer electron has been used for the development of a natural battery (Poddar and Khurana, 2011; Reguera et al., 2005). Even though the magnetite crystals produced by *Geobacter* are not uniform in their size, scientist who deals with these organisms in culture conditions are making substantial efforts to control the size of the magnetite to use them in medical purpose (Byrne et al., 2011).

Other indicator species in the magnetite–enriched samples may also play roles in magnetite formation or may favor the

environment rich in magnetite grain. These bacteria were phylogenetically diverse perhaps because they play a range of roles, or even if they perform the same role (iron reduction), they might not belong to a single phylum or class because of the long history of microbial iron reduction (Jimenez-Lopez et al., 2010; Lovley, 2013). Iron reduction has been suggested as the earliest form of microbial respiration (Lovley, 2013). Some of the bacterial species like *Geobacter* can obtain energy through iron reduction. Other bacterial species such as *Actinomucor repens*, *Bacillus mesentericus*, and *Escherichia coli*, or even some of archaeal species are able to reduce iron but unable to conserve energy through the process (Lovley, 2013). The groups of bacteria that are more common in the magnetite-enriched samples (Table 2), could be suggested as candidate magnetite formers, which have high potential to be studied for various purposes mentioned above in the case of *Geobacter*.

## 4.2. Micro-scale niche partitioning

Niche differentiation (also called as niche segregation, niche separation, and niche partitioning) has been studied mostly in a regional or in a local scale since the target species for the study were usually higher organisms rather than microbes. However, next generation sequencing has assisted studying micro-scale niche differentiation of microbes.

In this study, microbial community structure of one of the

samples from magnetite-enriched group was much more similar to the other magnetite-enriched samples, far apart more than 1 m away, than the magnetite-depleted sample gathered at the same point. This strongly suggests that microbes are able to find their own niche at a single grain scale and this can explain how the diverse soil microorganisms exist together.

Niche separation caused by type difference of minerals are not well studied so far. Magnetite is special in that it can be easily extracted using a powerful magnet. If this kind of study, separating one type of mineral and comparing the microbial community structure of the sample from depleted sample, could be applied to other types of mineral, it would be possible to get more evidence related to micro-scale niche separation and could be possible to understand its formation in biological perspective.

Some studies have reported micro-scale niche differentiation of microbes by separating different size of soil particles by sieving them (Sessitsch et al., 2001; Vos et al., 2013). Microbial biomass is usually high in fine-scale soil particle since the size of soil particle correlates with pore size (Kirchmann and Gerzabek, 1999; Sessitsch et al., 2001). Sessitsch et al. (Sessitsch et al., 2001) compared microbial community structure with different size of soil particles by using terminal restriction fragment length polymorphism (T-RFLP) method and found that the microbial community structure was distinctive with soil particle size and the microbial diversity was higher in small size fraction. In our study, the magnetite-enriched fraction had relatively small size of

granules compared to magnetite-depleted fraction which might in some extent affect the structure of microbial community.

## 5. Conclusions

This study demonstrated distinctive microbial community in relation to mineral composition, in this case, magnetite. The enrichment of *Geobacter* in magnetite-enriched group highly suggests their performance of iron reduction in real sediment soil, highlighting the point that the indicator species other than *Geobacter* including unculturable species in magnetite-enriched group might also play a similar role. However, to verify whether the candidate species are truly involved in magnetite formation, culture-based study is necessary.

The method used in this study, separating mineral by its type and comparing the microbial community structure with that of depleted sample, could also be applied to other types of mineral other than magnetite. This would help us to understand the biological formation of naturally occurring minerals.

## Publication

Song, H. K., Sonkaria, S., Khare, V., Dong, K., Lee, H. T., Ahn, S. H., Kim, H. K., Kang, H. J., Lee, S. H., Jung, S. P., and Adams, J. M. (2015). Pond Sediment Magnetite Grains Show a Distinctive Microbial Community. *Microbial ecology*, 1–7

## Bibliography

Aßhauer, K.P., Wemheuer, B., Daniel, R., and Meinicke, P. (2015). Tax4Fun: predicting functional profiles from metagenomic 16S rRNA data. *Bioinformatics*, *btv287*.

Amos, B.K., Sung, Y., Fletcher, K.E., Gentry, T.J., Wu, W.-M., Criddle, C.S., Zhou, J., and Löffler, F.E. (2007). Detection and quantification of *Geobacter lovleyi* strain SZ: implications for bioremediation at tetrachloroethene- and uranium-impacted sites. *Applied and environmental microbiology* *73*, 6898–6904.

Bazylinski, D.A., Frankel, R.B., and Konhauser, K.O. (2007). Modes of biomineralization of magnetite by microbes. *Geomicrobiology Journal* *24*, 465–475.

Blakemore, R. (1975). Magnetotactic bacteria. *Science* *190*, 377–379.

Bolger, A.M., Lohse, M., and Usadel, B. (2014). Trimmomatic: a flexible trimmer for Illumina sequence data. *Bioinformatics*, *btu170*.

Byrne, J., Telling, N., Coker, V., Patrick, R., van der Laan, G., Arenholz, E., Tuna, F., and Lloyd, J. (2011). Control of nanoparticle size, reactivity and magnetic properties during the bioproduction of magnetite by *Geobacter sulfurreducens*. *Nanotechnology* *22*, 455709.

Chun, J., Lee, J.-H., Jung, Y., Kim, M., Kim, S., Kim, B.K., and Lim, Y.-W. (2007). EzTaxon: a web-based tool for the identification of prokaryotes based on 16S ribosomal RNA gene sequences. *International Journal of Systematic and Evolutionary Microbiology* 57, 2259–2261.

Faulkner, S., Patrick, W., and Gambrell, R. (1989). Field techniques for measuring wetland soil parameters. *Soil Science Society of America Journal* 53, 883–890.

Goldhawk, D.E., Rohani, R., Sengupta, A., Gelman, N., and Prato, F.S. (2012). Using the magnetosome to model effective gene-based contrast for magnetic resonance imaging. *Wiley Interdisciplinary Reviews: Nanomedicine and Nanobiotechnology* 4, 378–388.

Greene, A.C., Patel, B.K., and Sheehy, A.J. (1997). *Deferribacter thermophilus* gen. nov., sp. nov., a novel thermophilic manganese- and iron-reducing bacterium isolated from a petroleum reservoir. *International journal of systematic bacteriology* 47, 505–509.

Jimenez-Lopez, C., Romanek, C.S., and Bazylinski, D.A. (2010). Magnetite as a prokaryotic biomarker: a review. *Journal of Geophysical Research: Biogeosciences* (2005–2012) 115.

Kirchmann, H., and Gerzabek, M.H. (1999). Relationship between soil organic matter and micropores in a long-term experiment at Ultuna, Sweden. *Journal of Plant Nutrition and Soil Science* 162, 493–498.

Lovley, D. (1995). Bioremediation of organic and metal contaminants with dissimilatory metal reduction. *Journal of Industrial Microbiology* 14, 85–93.

Lovley, D. (2013). Dissimilatory Fe(III)– and Mn(IV)–Reducing Prokaryotes. In *The Prokaryotes*, E. Rosenberg, E. DeLong, S. Lory, E. Stackebrandt, and F. Thompson, eds. (Springer Berlin Heidelberg), pp. 287–308.

Lovley, D.R., Stolz, J.F., Nord, G.L., and Phillips, E.J. (1987). Anaerobic production of magnetite by a dissimilatory iron–reducing microorganism. *Nature* 330, 252–254.

Masella, A.P., Bartram, A.K., Truszkowski, J.M., Brown, D.G., and Neufeld, J.D. (2012). PANDAseq: paired–end assembler for illumina sequences. *BMC bioinformatics* 13, 31.

Morgan, D. (2000). Separation, Magnetic Separation. In *Kirk–Othmer Encyclopedia of Chemical Technology* (John Wiley & Sons, Inc.).

Néel, L. (1955). Some theoretical aspects of rock–magnetism. *Advances in physics* 4, 191–243.

Nevin, K.P., Holmes, D.E., Woodard, T.L., Hinlein, E.S., Ostendorf, D.W., and Lovley, D.R. (2005). *Geobacter bemidjiensis* sp. nov. and *Geobacter psychrophilus* sp. nov., two novel Fe (III)–reducing subsurface isolates. *International Journal of Systematic and*

Evolutionary Microbiology *55*, 1667–1674.

Poddar, S., and Khurana, S. (2011). Geobacter: The Electric Microbe! Efficient Microbial Fuel Cells to Generate Clean, Cheap Electricity. *Indian journal of microbiology* *51*, 240–241.

Quast, C., Pruesse, E., Yilmaz, P., Gerken, J., Schweer, T., Yarza, P., Peplies, J., and Glöckner, F.O. (2012). The SILVA ribosomal RNA gene database project: improved data processing and web-based tools. *Nucleic acids research*, gks1219.

Reguera, G., McCarthy, K.D., Mehta, T., Nicoll, J.S., Tuominen, M.T., and Lovley, D.R. (2005). Extracellular electron transfer via microbial nanowires. *Nature* *435*, 1098–1101.

Schloss, P.D., Westcott, S.L., Ryabin, T., Hall, J.R., Hartmann, M., Hollister, E.B., Lesniewski, R.A., Oakley, B.B., Parks, D.H., and Robinson, C.J. (2009). Introducing mothur: open-source, platform-independent, community-supported software for describing and comparing microbial communities. *Applied and environmental microbiology* *75*, 7537–7541.

Sessitsch, A., Weilharter, A., Gerzabek, M.H., Kirchmann, H., and Kandeler, E. (2001). Microbial population structures in soil particle size fractions of a long-term fertilizer field experiment. *Applied and Environmental Microbiology* *67*, 4215–4224.

Su, D., Horvat, J., Munroe, P., Ahn, H., Ranjbartoreh, A.R., and

Wang, G. (2012). Polyhedral magnetite nanocrystals with multiple facets: Facile synthesis, structural modelling, magnetic properties and application for high capacity lithium storage. *Chemistry–A European Journal* *18*, 488–497.

Vo, N.X.Q., and Kang, H. (2013). Regulation of soil enzyme activities in constructed wetlands under a short-term drying period. *Chemistry and Ecology* *29*, 146–165.

Vos, M., Wolf, A.B., Jennings, S.J., and Kowalchuk, G.A. (2013). Micro-scale determinants of bacterial diversity in soil. *FEMS microbiology reviews* *37*, 936–954.

# APPENDIX

## Mothur commend line

```
make.group(fasta=D1.fasta-D2.fasta-D3.fasta-D4.fasta-M1.fasta-M2.fasta-M3.fasta-M4.fasta, groups=D1-D2-D3-D4-M1-M2-M3-M4)
```

```
unique.seqs(fasta=magnetite.fasta)
```

```
summary.seqs(fasta=current, name=current)
```

```
align.seqs(fasta=current, reference=silva.nr_v119.align, flip=t, processors=8)
```

```
summary.seqs(fasta=current, name=magnetite.names, processors=8)
```

```
screen.seqs(fasta=magnetite.unique.align, name=magnetite.names, group=magnetite.groups, maxhomop=6, end=13858, maxambig=0, optimize=start, criteria=95, processors=8)
```

```
summary.seqs (fasta=current, name=current)
```

```
filter.seqs (fasta=magnetite.unique.good.align, vertical=t, trump=., processors=8)
```

```
summary.seqs (fasta=current, name=current)
```

```
unique.seqs (fasta=magnetite.unique.good.filter.fasta, name=magnetite.good.names)
```

```
pre.cluster (fasta=magnetite.unique.good.filter.unique.fasta, name=magnetite.unique.good.filter.names,  
group=magnetite.good.groups, diffs=2, processors=1)
```

```
summary.seqs (fasta=current, name=current)
```

```
chimera.uchime (fasta=magnetite.unique.good.filter.unique.precluster.fasta,  
name=magnetite.unique.good.filter.unique.precluster.names, group=magnetite.good.groups)
```

```
remove.seqs (accnos=magnetite.unique.good.filter.unique.precluster.uchime.accnos,  
fasta=magnetite.unique.good.filter.unique.precluster.fasta,
```

```
name=magnetite.unique.good.filter.unique.precluster.names, group=magnetite.good.groups)

summary.seqs(fasta=current, name=current)

classify.seqs(fasta=magnetite.unique.good.filter.unique.precluster.pick.fasta,
name=magnetite.unique.good.filter.unique.precluster.pick.names, group=magnetite.good.pick.groups,
template=eztaxon_unaligned_20130408.fasta, taxonomy=eztaxon.taxonomy, cutoff=80, iters=1000)

remove.lineage(fasta=magnetite.unique.good.filter.unique.precluster.pick.fasta,
taxonomy=magnetite.unique.good.filter.unique.precluster.pick.eztaxon.wang.taxonomy,
name=magnetite.unique.good.filter.unique.precluster.pick.names, group=magnetite.good.pick.groups,
taxon=Chloroplast-Mitochondria-unknown-Archaea-Eukaryota)

system(cp magnetite.unique.good.filter.unique.precluster.pick.pick.fasta magnetite_final.fasta)

system(cp magnetite.unique.good.filter.unique.precluster.pick.pick.names magnetite_final.names)

system(cp magnetite.good.pick.pick.groups magnetite_final.groups)
```

```
system(cp magnetite.unique.good.filter.unique.precluster.pick.eztaxon.wang.pick.taxonomy magnetite_final.taxonomy)

dist.seqs(fasta=magnetite_final.fasta, cutoff=0.2, processors=1)

cluster(column=magnetite_final.dist, name=magnetite_final.names, method=average)

split.abund(fasta=magnetite_final.fasta, list=magnetite_final.an.list, group=magnetite_final.groups, cutoff=1,
label=0.03)

list.seqs(list=magnetite_final.an.0.03.rare.list)

remove.seqs(fasta=magnetite_final.fasta, name=magnetite_final.names, group=magnetite_final.groups,
taxonomy=magnetite_final.taxonomy, accnos=magnetite_final.an.0.03.rare.accnos, dups=f)

list.seqs(name=magnetite_final.pick.names)

get.seqs(accnos=magnetite_final.pick.accnos, list=magnetite_final.an.0.03.abund.list)
```

```
make.shared(list=magnetite_final.an.0.03.abund.pick.list, group=magnetite_final.pick.groups, label=0.03)
```

```
classify.otu(taxonomy=magnetite_final.pick.taxonomy, name=magnetite_final.pick.names,  
list=magnetite_final.an.0.03.abund.pick.list, group=magnetite_final.pick.groups, label=0.03)
```

```
sub.sample(shared=magnetite_final.an.0.03.abund.pick.shared)
```

```
rarefaction.single(shared=magnetite_final.an.0.03.abund.pick.0.03.subsample.shared, freq=50)
```

**Table A1** Functional characterization of magnetite-depleted (D) and magnetite-enriched (M). Only the top 50 most dominant functions are shown

<b>Function</b>	<b>D (%)</b>	<b>M (%)</b>	<b>M/D</b>
Flagellar assembly	1.082	1.267	1.171
Bacterial secretion system	1.780	2.051	1.153
Bacterial chemotaxis	1.339	1.534	1.146
Lipopolysaccharide biosynthesis	0.895	0.985	1.101
Two-component system	9.123	9.845	1.079
Cell cycle – Caulobacter	1.430	1.539	1.076
Nitrogen metabolism	2.100	2.220	1.057
Oxidative phosphorylation	1.935	2.007	1.037
Phenylalanine metabolism	0.695	0.718	1.033
Glyoxylate and dicarboxylate metabolism	1.249	1.282	1.026
Biotin metabolism	0.641	0.658	1.026
Carbon fixation pathways in prokaryotes	1.047	1.071	1.023
Porphyrin and chlorophyll metabolism	1.774	1.809	1.020
Mismatch repair	0.929	0.946	1.018
Citrate cycle (TCA cycle)	0.657	0.669	1.018
Lysine degradation	0.601	0.608	1.011
RNA degradation	1.334	1.347	1.010
Arginine and proline metabolism	1.703	1.719	1.009
Nicotinate and nicotinamide metabolism	0.738	0.742	1.005
Glutathione metabolism	0.756	0.759	1.004
Phenylalanine, tyrosine and tryptophan biosynthesis	1.047	1.051	1.003
Homologous recombination	1.169	1.170	1.001

Valine, leucine and isoleucine degradation	0.780	0.780	1.000
Cysteine and methionine metabolism	1.079	1.078	0.999
Alanine, aspartate and glutamate metabolism	1.086	1.084	0.999
Glycerophospholipid metabolism	0.891	0.889	0.998
Glycine, serine and threonine metabolism	1.375	1.372	0.998
Aminoacyl-tRNA biosynthesis	2.659	2.650	0.997
Ubiquinone and other terpenoid-quinone biosynthesis	0.743	0.741	0.996
Histidine metabolism	0.799	0.792	0.992
Base excision repair	0.634	0.629	0.991
Nucleotide excision repair	1.060	1.051	0.991
Pantothenate and CoA biosynthesis	0.649	0.643	0.990
Ribosome	1.525	1.509	0.990
Purine metabolism	3.115	3.076	0.988
Pyrimidine metabolism	1.975	1.949	0.987
Butanoate metabolism	0.861	0.849	0.987
Pyruvate metabolism	1.248	1.227	0.983
Fatty acid biosynthesis	0.761	0.747	0.981
Lysine biosynthesis	0.868	0.850	0.980
Peptidoglycan biosynthesis	1.339	1.309	0.978
Methane metabolism	1.514	1.474	0.974
Terpenoid backbone biosynthesis	0.771	0.747	0.970
Benzoate degradation	0.629	0.610	0.969
ABC transporters	7.225	6.890	0.954
Pentose phosphate pathway	0.898	0.846	0.942
Amino sugar and nucleotide sugar metabolism	1.908	1.796	0.941
Glycolysis / Gluconeogenesis	0.811	0.759	0.936

Starch and sucrose metabolism	2.041	1.903	0.932
Fructose and mannose metabolism	1.324	1.216	0.918

## 국문초록 (Abstract in Korean)

자철석은 자연계에 존재하는 광물 중 하나로 페리 자성 (ferrimagnetic property)을 띤다. 이화적 철 환원작용(dissimilatory iron reduction)을 통해 자철석을 형성하는 박테리아 종은 그 응용 분야가 다양하기 때문에 배양 조건에서의 연구가 많이 진행되어 왔다. 그러나 생태학적 측면에서 보았을 때 그들이 실제 자연계에서도 자철석 형성에 기여하는지에 관해서는 거의 밝혀진 바가 없다.

이에 본 연구는 배양 비의존적 차세대 염기서열 분석(next generation sequencing)기술을 이용하여 담수 연못 퇴적토 내 자철석 입자에 착생하는 미생물 군집 구조를 알아보는 것을 목적으로 수행되었다. 연못에서 채취한 퇴적토 샘플은 자석을 이용하여 자철석이 많이 함유된 부분과 자철석이 거의 없는 부분으로 나뉘었다. 각 부분에서 추출된 DNA는 박테리아의 16S 리보솜 RNA 유전자를 대상으로 증폭된 후 차세대 염기서열 분석 기술을 이용하여 시퀀싱(sequencing)되었다.

자철석이 많이 함유된 부분과 거의 없는 부분의 미생물 군집 구조를 비교 분석한 결과 두 구조는 상이했으며, 자철석이 다량 함유된 부분에서 가장 많이 발견된 OTU(operational taxonomic unit, 97% 염기서열 유사도를 바탕으로 하나의 종이 정의됨)가 배양 조건에서 자철석을 형성하는 것으로 널리 알려져 있는 지오박터(*Geobacter*)에 속하는 것으로 밝혀졌다. 해당 OTU 외에도 자철석이 거의 없는 부분과 비교했을 때 자철석이 다량 함유된 부분에 특별히 많이 포함되어 있는 박테리아 종들이 있었으며, 이는 자철석 형성 박테리아로서의 그들의 잠재성을 보여주는 결과였다. 또한 본 연구 결과는 극히 적은 양의 토양 내에서도 광물 질의 종류에 따라 분서(niche differentiation)가 일어날 수 있음을 보여주었다.

주요어: 자철석, 지오박터, 차세대 염기서열 분석, 박테리아 16S 리보솜  
RNA 유전자, 분석  
학번: 2014-20313